Probing the Coordination Chemistry of $[Zr_6BCl_{12}]^+$: A Cluster Especially Amenable to NMR Study

Xiaobing Xie, Joseph H. Reibenspies, and Timothy Hughbanks*

Contribution from the Department of Chemistry, Texas A&M University, P.O. Box 300012, College Station, Texas 77842-3012

Received May 18, 1998

Abstract: NMR spectroscopy is demonstrated to be a powerful analytical tool for the study of solvolysis and ligand-exchange chemistry of the $[Zr_6BCl_{12}]^+$ cluster in acetonitrile, methanol, and pyridine. ^{11}B NMR spectra for $[(Zr_6BCl_{12})Cl_{6-x}L_x]^{x-5}$ (L = CH_3CN, CH_3OH, and pyridine; $x = 1-6$) are reported. Exceedingly narrow ^{11}B lines are generally observed for these clusters. Two-bond ($^2J_{P-Zr-B} = 8.8$ Hz) and three-bond coupling constants ($^3J_{P-O-Zr-B} = 1.9$ Hz) are observed for the cluster complexes $[(Zr_6BCl_{12})(PR_3)_6]^+$ and $[(Zr_6BCl_{12})(OPR_3)_xL_{6-x}]^+$ (L = CH_3CN and PR_3), respectively, in both ^{11}B and ^{31}P NMR spectra. Spin−lattice relaxation times (T_1's) for ^{11}B were measured for several cluster complexes. Homoleptic species, $[(Zr_6BCl_{12})L_6]^+$ (L = CH_3CN, CH_3OH, pyridine), exhibit very long times and that for $[(Zr_6BCl_{12})(NCCH_3)_6]^+$ is the longest ever measured ($T_1 = 108$ s) for the ^{11}B nucleus. A thermodynamic analysis of spectra for the $[(Zr_6BCl_{12})(CH_3OH)_{6-x}(py)_x]^+$ ($x = 0-5$) system reveals that $[Zr_6BCl_{12}]^+$ binds pyridine more strongly than methanol by about 3 kJ/mol. Crystallographic structural analyses of $[(Zr_6BCl_{12})Cl(py)_5]\cdot 3CH_3CN$ and [pyH]{*cis*-$[(Zr_6BCl_{12})Cl_2(py)_4]$}·3py are also reported. The following parameters were determined for these two compounds: $[(Zr_6BCl_{12})Cl(py)_5]\cdot 3CH_3CN$, orthorhombic, *Pbcm*, $a = 13.4268(1)$ Å, $b = 25.8258(1)$ Å, $c = 14.5918(2)$ Å, $Z = 4$; [pyH]{*cis*-$[(Zr_6BCl_{12})Cl_2(py)_4]$}·3py, monoclinic, *C*2/*c*, $a = 14.5999(3)$ Å, $b = 21.2298(5)$ Å, $c = 19.8292(5)$ Å, $\beta = 101.892(1)°$, $Z = 4$.

Introduction

Nuclear magnetic resonance (NMR) spectra of quadrupolar nuclei in highly symmetric environments exhibit dramatically narrowed lines because quadrupolar broadening does not occur when the electric field gradient at the nucleus vanishes. While such narrowed lines are pleasing and quite characteristic when they occur, the high symmetry required for their observation (cubic or icosahedral point symmetries) generally precludes the exploitation of such line narrowing for analytical purposes. Since chemical variability goes hand-in-hand with structural asymmetry, such variability usually generates electronic asymmetry, nonzero electric field gradients, and quadrupolar broadening of NMR lines for nuclei that are not spin-$^1/_2$. In our laboratories we have been studying a class of centered hexanuclear zirconium halide clusters, $[(Zr_6ZCl^i_{12})L^a_6]^{m-}$ (Z = H, Be, B, C, N, Mn, Fe, and Co), for which this disappointing compromise (for quadrupolar Z) between analytical breadth and spectral resolution seems to be largely avoidable.

The solution chemistry of $[(Zr_6ZCl^i_{12})L^a_6]^{m-}$ clusters has undergone extensive study in our laboratory for the past few years. Initial work by Rogel and Corbett[1−3] showed that several of these clusters, $[(Zr_6ZCl_{12})]^{n+}$ (Z = H, Be, B, C, and Fe), could be extracted intact from solid-state precursors into acetonitrile solution. Research in our laboratory[4−7] has demonstrated that aluminum trichloride/1-ethyl-3-methylimidazolium chloride ($ImCl/AlCl_3$) room temperature molten salts can effectively dissolve numerous centered zirconium halide cluster compounds. Until recently, however, two obstacles to the efficient development of this solution chemistry have been the nearly exclusive reliance on crystallography as a means of characterization and the limited number of solvents available for dissolving the solid-state precursors.

Of the known $[(Zr_6ZCl^i_{12})L^a_6]^{m-}$ clusters, nearly all of the known interstitials (Z) have NMR-active isotopes. We have therefore set out to establish systematic measurements to enable routine use of NMR spectroscopy as an analytical tool in studying this chemistry. We recently reported our use of NMR to monitor these clusters' solution chemistry[8] and demonstrated the feasibility for such investigation, with special attention given to ^{13}C centered clusters.

$Rb_5Zr_6Cl_{18}B$ serves as a convenient source of boron-centered clusters for solution chemistry. The clusters in this compound are discrete in the solid, and because there is no bridging between clusters occurs,[9] dissolution of the clusters occurs under mild conditions. We show here that investigation of the boron-centered cluster may be extended beyond acetonitrile and molten salts ($ImCl/AlCl_3$) to include other polar solvents such as methanol and pyridine. In this paper, we present our systematic studies of the $[Zr_6BCl_{12}]^+$ cluster core in acetonitrile, methanol,

* To whom correspondence should be addressed.

(1) Rogel, F.; Corbett, J. D. *J. Am. Chem. Soc.* **1990**, *112*, 8198−8200.
(2) Rogel, F.; Zhang, J.; Payne, M. W.; Corbett, J. D. In *Electron Transfer in Biology and the Solid State*; Johnson, M. K., King, R. B., Kurtz D. M., Jr., Kutal, C., Norton, M. L., Scott, R. A., Eds.; American Chemical Society: Washington, DC, 1990; Vol. 226, pp 367−389.
(3) Rogel, F. Ph.D. Thesis, Iowa State University, 1990.
(4) Runyan, C. E., Jr. Ph.D. Thesis, Texas A&M University, 1994.
(5) Runyan, C. E., Jr.; Hughbanks, T. *J. Am. Chem. Soc.* **1994**, *116*, 7909−7910.
(6) Tian, Y.; Hughbanks, T. *Inorg. Chem.* **1995**, *34*, 6250−6254.
(7) Tian, Y.; Hughbanks, T. *Z. Anorg. Allg. Chem.* **1996**, *622*, 425−431.
(8) Harris, J. D.; Hughbanks, T. *J. Am. Chem. Soc.* **1997**, *119*, 9449−9459.
(9) Ziebarth, R. P.; Corbett, J. D. *J. Am. Chem. Soc.* **1989**, *111*, 3272−3280.

10.1021/ja981736n CCC: $15.00
Published on Web 10/22/1998

Table 1. Sample Preparation for NMR Measurement from the Solid-State Precursor, $Rb_5Zr_6Cl_{18}B$

no.	additional reactants	solvents	reaction time[a]	parameters used for T1 measurements
1	none	CD_3CN	14 days	NA
2	6 equiv of $TlPF_6$	CD_3CN	14 h	180° pulse width, 68 μs; 90° pulse width, 34 μs; delay, 600 s
3	10 equiv of PPNCl	CD_3CN	14 h	NA
4	none	CD_3OD	1 h	180° pulse width, 64 μs; 90° pulse width, 32 μs; delay, 100 s
5	6 equiv of $TlPF_6$	CD_3OD	1 h	NA
6	none	pyridine	3 days	NA
7	none	pyridine	7 days (120 °C)	180° pulse width, 50 μs; 90° pulse width, 25 μs; delay, 1.5 s
8	6 equiv of $TlPF_6$	pyridine	2 days	180° pulse width, 68 μs; 90° pulse width, 34 μs; delay, 180 s
9	6 equiv of $TlPF_6$	(a) CD_3OD (b) 0.4 mL pyridine	1 h	180° pulse width, 64 μs; 90° pulse width, 32 μs; delay, 80 s (20 °C), 40 s (−20 °C)
10	6 equiv of $TlPF_6$ (b) 0.02 mL of pyridine	(a) CD_3CN	14 h	NA
11	(a) 6 equiv of $TlPF_6$, 6 equiv of PEt_3	(a) CH_3CN (b) dried in vacuo (c) CH_2Cl_2	14 h	NA
12	(a) 6 equiv of $TlPF_6$ (b) 6 equiv of $OPPh_3$	pyridine	14 h	NA

[a] 20 °C for all samples except No. 7.

and pyridine, with attention given to solvolysis, thermodynamics of ligand exchange, and measurements of ^{11}B spin−lattice relaxation times.

The most important and novel feature of this study is the manner in which NMR spectroscopy serves in a more central and comprehensive analytical role in the study of $[Zr_6BCl_{12}]^+$-based clusters than is possible for any other polynuclear clusters of the early transition metals. This fact derives from the fortunate confluence of two circumstances. First, the electronic environment immediately surrounding the boron atom has nearly octahedral symmetry and the electric field gradient at the nucleus is small enough that quadrupolar broadening of ^{11}B resonances is virtually negligible. Spectra presented in this paper demonstrate that this is true even when the distribution of ligands (L) on the cluster exterior is quite asymmetric. Second, the central boron nucleus is still sensitive enough to the ligands on the exterior of the cluster to be an excellent "reporter" of their presence via changes in chemical shift and spin−spin coupling. Thus, within the class of boron-centered hexanuclear zirconium clusters, ^{11}B NMR spectroscopy has very high resolution, good sensitivity, a chemical shift range with useful breadth, and interpretive simplicity.

Experimental Section

Techniques and Materials. Manipulation of all compounds was performed either in an inert atmosphere (N_2) glovebox or on Schlenk (Ar) or high-vacuum lines. All glassware and syringe needles were oven dried (160 °C) overnight before use.

The cluster precursor material, $Rb_5Zr_6Cl_{18}B$, was synthesized in a manner previously reported: stoichiometric proportions of RbCl (Alfa), $ZrCl_4$ (Aldrich), Zr powder and boron (Alfa) powder were sealed in a Nb tube, which is sealed under vacuum in a fused silica jacket and heated at 850 °C for 2−4 weeks.[9] Synthesis of $Rb_5Zr_6Cl_{18}B$ is confirmed by Guinier X-ray powder diffraction. RbCl and $ZrCl_4$ were sublimed under vacuum prior to use. Zr powder is prepared from Zr foil by a hydrogenation−dehydrogenation reaction that has been described previously.[10] Boron powder was used as received.

Nondeuterated acetonitrile (spectroscopic grade, Aldrich), pyridine (Aldrich), dichloromethane (EM), and triethylphosphine (Aldrich) were dried by refluxing over calcium hydride overnight and then distilling under nitrogen before use. Methanol was dried over sodium methoxide overnight and then distilled under N_2 before use. Deuterated methanol (CIL) was dried by refluxing with $NaOCH_3$ overnight and then transferred to a storage flask by vacuum distillation. Deuterated acetonitrile (CIL) was purified by refluxing over phosphorus pentoxide. All deuterated solvents were stored in a nitrogen glovebox. Thallium triflate (Strem), thallium hexafluorophosphate (Strem), and triphenylphosphine oxide (Aldrich) were used as received. Triphenylphosphine was vacuum sublimed before use. Bis(triphenylphosphine)-iminium chloride (PPNCl) (Aldrich) was recrystallized three times from acetone with diethyl ether before use.

NMR. Solution NMR spectra were measured on a Varian XL 200 broad-band spectrometer (^{11}B at 64.18 MHz, ^{31}P at 80.98 MHz). Spectra were measured in CD_3CN and CD_3OD in 10 mm NMR tubes with typical sample volumes of 3−5 mL. In the case of pyridine or dichloromethane solutions, a coaxial inner tube with deuterated benzene (C_6D_6) was used to lock the signals. Chemical shifts for ^{11}B and ^{31}P were reported with respect to the external standards $BF_3{\cdot}OEt_2$ and H_3PO_4, respectively ($\delta = 0$). In most cases, acquisition times of 2.5 s were used. 1000−5000 transients were usually required to obtain reasonably good signal-to-noise ratios. The spin−lattice relaxation time (T_1's) for ^{11}B were determined for several cluster species with the standard inversion recovery technique.[11] The standard VNMR software package[12] was utilized to analyze the data.

Preparation of the NMR Solutions. In most cases, a mixture of reactants ($Rb_5Zr_6Cl_{18}B$, and $TlPF_6$ or PPNCl) and a stir bar were loaded in an ampule, solvent was added with a syringe, and the ampule was sealed on a Schlenk line. The mixtures were stirred until no further dissolution of the reactants was apparent (1 day or more in CD_3CN or pyridine, only an hour in CD_3OD), solids were removed by centrifugation, and the orange-red solutions was transferred to NMR tubes. When CD_3CN or pyridine is used as the solvent, a significant fraction of the original solids does not dissolve. Details concerning sample preparations are summarized in Table 1.

X-ray Structure Determinations. Single-crystal structure determinations were undertaken for two of the cluster complexes with the $[Zr_6BCl_{12}]^+$ core. In each case, a crystal was mounted immediately after being in contact with the mother solution. Crystals were coated with Apiezon-T stopcock grease, mounted on the tip of glass fibers, and immediately inserted into the low-temperature nitrogen stream of the diffractometer for data collection. Data were collected at −60 °C using a Siemens (Bruker) SMART CCD (charge coupled device) equipped diffractometer with a LT-2 low-temperature apparatus. For both crystals, data were measured with omega scans of 0.3° per frame for 30 s, such that a hemisphere was collected. A total of 1271 frames were collected with a maximum resolution of 0.75 Å. The first 50 frames were recollected at the end of data collection to monitor for decay. Cell parameters were retrieved with SMART software[13] and refined with SAINT software[14] on all observed reflections. Data reduction was performed with SAINT, which corrects for Lorentz

(10) Smith, J. D.; Corbett, J. D. *J. Am. Chem. Soc.* **1985**, *107*, 5704−5711.

(11) Vold, R. L.; Waugh, J. S.; Klein, M. P.; Phelps, D. E. *J. Chem. Phys.* **1968**, *48*, 3831−3832.

(12) VNMR V5.3b: *Varian NMR software*; Varian, 1996.

(13) SMART V4.043: *Software for the CCD Detector System*; Bruker Analytical X-ray System: Madison, WI, 1995.

(14) SAINT V4.035: *Software for the CCD Detector System*; Bruker Analytical X-ray System: Madison, WI, 1995.

Table 2. Crystallographic Data for Centered Zirconium Chloride Cluster Complexes

	$[(Zr_6BCl_{12})Cl(py)_5]\cdot 3CH_3CN$	$[pyH]\{cis\text{-}[(Zr_6BCl_{12})Cl_2(py)_4]\}\cdot 3py$
chem formula	$C_{31}H_{25}BCl_{13}N_8Zr_6$	$C_{40}H_{30}BCl_{14}N_8Zr_6$
fw	1528.57	1677.15
space group	*Pbcm* (No. 57)	*C*2/*c* (No. 15)
a, Å	13.4268(2)	14.5999(3)
b, Å	25.8258(1)	21.2298(5)
c, Å	14.5918(2)	19.82929(5)
β, deg		101.892(1)
V, Å^3	5059.82(10)	6014.2(2)
Z	4	4
ρ_{calcd}, g cm^{-3}	2.007	1.852
μ, mm^{-1}	1.911	1.660
λ, radiation (Mo), Å	0.71073	0.71073
T, °C	−60.0	−60.0
GOF	1.21	1.14
R(F)[a]	0.0625	0.0455
wR(F^2)[b]	0.1038	0.0863

[a] $R(F) = \sum||F_o| - |F_c||/\sum|F_o|$. [b] $wR(F^2) = [\sum[w(F_o^2 - F_o^2)^2]/\sum[w(F_o^2)^2]]^{0.5}$.

polarization and decay. Absorption corrections were applied with SADABS[15] supplied by George Sheldrick. The structures were solved by use of direct methods with the SHELXS-97 program[16] and refinement was performed by the least-squares method on F^2 with the SHELXL-97 package,[17] incorporated in SHELXTL-PC V5.03.[18] Pertinent crystallographic data for both compounds are listed in Table 2.

(a) $[(Zr_6BCl_{12})Cl(py)_5]\cdot 3CH_3CN$. An acetonitrile solution of $[(Zr_6BCl_{12})(NCCH_3)_6]^+$ to which 0.02 mL of pyridine had been added was put into a capped vial and stored in a nitrogen glovebox for 3 days. Dark red crystals, along with some gray precipitate, were observed to have grown from the original red solution. One such crystal ($0.15 \times 0.10 \times 0.05$ mm^3) was mounted in the manner described above and data were collected. A total of 22863 reflections were collected, of which 5692 were unique ($R_{int} = 0.0649$) and 3922 were observed with $I \geq 2\sigma(I)$. The space groups *Pbcm* and *Pbc*2_1 were consistent with the observed systematic absences; *Pbcm* was chosen on the basis of the form of the distribution of intensities. All the non-hydrogen atoms associated with the cluster were refined with anisotropic thermal parameters. Idealized hydrogen positions on the pyridine ligands were calculated and placed in the refinement with the C−H distance equal to 0.94 Å. A model of three disordered acetonitrile solvent molecules with fixed C_a-C_b (1.423 Å), C_a-N (1.146 Å), and $C_b\cdots N$ (2.569 Å) distances was introduced. The final cycle of the full-matrix least-squares refinement was based on 3922 observed reflections, 9 restraints, and 270 parameters, and converged with unweighted and weighted agreement factors of *R(F)* = 0.0625 and *wR*(F^2) = 0.1038, respectively. The largest residual peak and hole are 1.3 e/Å^3 and −0.9 e/Å^3, respectively.

(b) $[pyH]\{cis\text{-}[(Zr_6BCl_{12})Cl_2(py)_4]\}\cdot 3py$. A few red crystals were obtained when $Rb_5Zr_6Cl_{18}B$ was heated in pyridine at 120 °C in a sealed ampule. A dark red plate ($0.15 \times 0.15 \times 0.035$ mm^3) was mounted in the manner described above and data were collected. A total of 13947 reflections were collected, of which 6086 were unique ($R_{int} = 0.0398$) and 4487 were observed with $I \geq 2\sigma(I)$. All the non-hydrogen atoms associated with the cluster were refined with anisotropic thermal parameters. Idealized hydrogen positions on the pyridine ligands were calculated and placed in the refinement with the C−H distance equal to 0.94 Å. One of the free pyridine molecules was located directly from the electron density difference map and refined anisotropically. It seemed that another pyridine molecule was severely disordered in a void. A model with two constrained carbon hexagons, each oriented independently and having a 0.5 site occupancy factor, was introduced to accommodate electron density peaks in the void. Atoms in both rigid rings were refined isotropically. Hydrogen "riding atoms" were not added on these disordered pyridine molecules. The final cycle of the full-matrix least-squares refinement was based on 4487 observed reflections and 249 parameters, and converged with unweighted and weighted agreement factors of *R(F)* = 0.0455 and *wR*(F^2) = 0.0863, respectively. The largest residual peak and hole are 0.8 e/Å^3 and −0.6 e/Å^3, respectively.

Results and Discussion

The development of the coordination chemistry of the molecular cluster complexes has been heavily reliant on single crystal X-ray diffraction for detailed characterization. Although crystallography can provide conclusive identification of product when single crystals of a product are obtained, quite often the composition of the mother solution is different from crystals obtained therefrom, since the crystalline product is often just the least soluble of the species present. With notable exceptions, crystallography has been by far the dominant characterization technique in studying hexanuclear clusters of the early transition elements (e.g., $[Mo_6X_8]^{n+}$, $[(Nb,Ta)_6X_{12}]^{m+}$, $[Re_6Ch_8]^{2+}$; X = halogen, Ch = chalcogen).

As is the case in transition metal chemistry generally, NMR spectra with ligand nuclei (e.g., ^{13}C, ^{31}P, ^{19}F) can be used to monitor reactions of hexanuclear clusters. For example, Holm and co-workers have recently used ^{31}P NMR spectra to identify the presence of $[Re_6S_8(PEt_3)_{6-x}Br_x]^{2-x}$ cluster species in solution, assess the phosphine−bromide distributions (x), and identify isomeric species.[19] Similarly, ^{19}F NMR was used by Preetz and co-workers to study the ligand exchange reactions of $[(Mo_6Cl_8)F_6]^{2-}$ with $[(Mo_6Cl_8)X_6]^{2-}$ (X = Cl, Br, I) in acetonitrile and the mixed cluster ions, $[(Mo_6Cl_8)F_nX_{6-n}]^{2-}$ (n = 1−6).[20] Species were characterized by their distinct ^{19}F NMR chemical shifts and statistical distributions of geometric isomers were observed.[20] Such studies are, of course, limited to ligands with appropriate nuclei, and those nuclei must be sufficiently influenced by remotely bound ligands that they serve as an appropriate probe of the cluster's environment. Alternatively, one can study the NMR spectra for the metal nuclei that comprise the cluster itself. ^{95}Mo NMR has been used for limited studies of Mo_6X_8-based clusters and some chemical shift correlations have been established.[21−23] In general, however, low magnetogyric ratios and/or natural abundances and large quadrupole moments limit the range of usefulness of NMR spectra for most metals.

We have shown that the presence of interstitial atoms in hexanuclear zirconium clusters offers the prospect of using multinuclear NMR to monitor the coordination chemistry of these clusters.[8] ^{11}B is a useful nucleus for NMR study because of its high abundance, high detection sensitivity, and relatively small quadrupole moment. Generally, ^{11}B NMR spectra consist of lines that are not so broad that they are uninformative, but line widths for ^{11}B resonances are still typically greater than

(15) SADABS: *Program for absorption corrections using Siemens CCD based on the method of Robert Blessing*; Blessing, R. H. *Acta Crystallogr.* **1995**, *A51*, 33−38.

(16) SHELXS-90: Sheldrick, G. M. *Program for the Solution of Crystal Structure*; University of Göttingen, Germany, 1990.

(17) SHELXL-97: Sheldrick, G. M. *Program for the Refinement of Crystal Structure*, University of Göttingen, Germany, 1997.

(18) SHELXTL 5.10 (PC-Version): *Program library for Structure Solution and Molecular Graphics*; Bruker Analytical X-ray Systems: Madison, WI, 1998.

(19) Willer, M. W.; Long, J. R.; McLauchlam, C. C.; Holm, R. H. *Inorg. Chem.* **1998**, *37*, 328−333.

(20) Harder, K.; Peters, G.; Preetz, W. *Z. Anorg. Allg. Chem.* **1991**, *598/599*, 139−149.

(21) Ebihara, M.; Toriumi, K.; Saito, K. *Inorg. Chem.* **1988**, *27*, 13−18.

(22) Preetz, W.; Bublitz, D.; Von Schnering, H. G.; Saβmannshausen, J. *Z. Anorg. Allg. Chem.* **1994**, *620*, 234−246.

(23) Granger, P. In *Advanced Application of NMR to Organometallic Chemistry*; Gielen, M., Willem, R., Wrackmeyer, B., Eds.; John Wiley & Sons: Chichester, 1996.

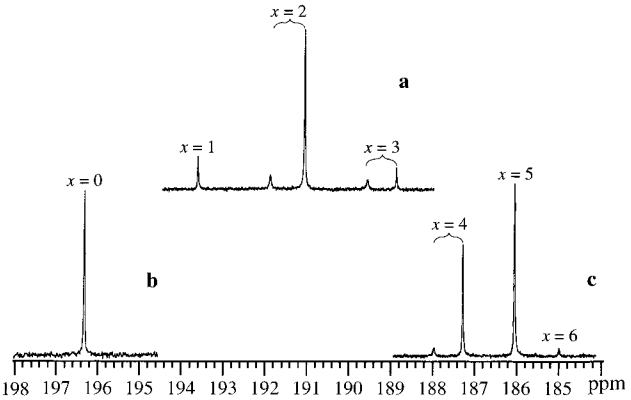

Figure 1. ^{11}B NMR spectra for $Rb_5Zr_6Cl_{18}B$ dissolved in acetonitrile with (a) no added ligand, (b) 6 equiv of added $TlPF_6$, and (c) 10 equiv of added PPNCl. Labeling on the peaks ($x = 0-6$) indicates the number of terminal chlorides in $[(Zr_6BCl_{12})(NCCH_3)_{6-x}Cl_x]^{1-x}$.

10 Hz. However, because the boron atom in a $[Zr_6BCl_{12}]^+$ cluster resides in a nearly octahedral environment, remarkably narrow lines (0.3−3.0 Hz) are observed in the ^{11}B NMR spectra of these cluster complexes. We are therefore able to use ^{11}B NMR spectroscopy as a routine analytical tool to study the speciation, coupling, and ligand exchange of these zirconium cluster complexes in solution.

(a) Speciation in Different Solvents. In our investigation of the coordination chemistry of the $[Zr_6BCl_{12}]^+$ cluster, acetonitrile, methanol, and pyridine have been extensively used as solvents for excising the cluster from the solid state. These three solvents all have relatively high dielectric constants, and the ionic solid-state precursor, $Rb_5Zr_6Cl_{18}B$, has reasonable solubility in these solvents at room temperature. The clusters can therefore be extracted into solutions without much difficulty. Organic solvents with lower dielectric constants, such as THF, hexane, dichloromethane, and toluene, fail to dissolve any known zirconium cluster compound even at elevated temperature.

(i) Cluster in Acetonitrile. Corbett and co-workers found[1,3] that $Rb_5Zr_6Cl_{18}B$ could be dissolved in acetonitrile forming a light orange red solution with the cluster core, $[(Zr_6BCl_{12})]^+$, remaining intact in the solution. However, the solvolysis and ligand-binding properties of this cluster in solution remained unexplored. When $Rb_5Zr_6Cl_{18}B$ was stirred in neat acetonitrile for 6 days, a light orange red solution was formed, and a significant fraction of the original solids do not dissolve. This phenomenon does not necessarily reflect saturation of the solution though, since the addition of fresh solids yields more concentrated solutions. Powder diffraction data indicate that the undissolved solids are mainly starting materials so we presume that some sort of surface blockage eventually inhibits dissolution of $Rb_5Zr_6Cl_{18}B$. In the ^{11}B NMR spectrum of the red solution, a series of five singlets was observed with the chemical shifts of 193.8, 192.1, 191.2, 189.7, and 189.0 ppm (Figure 1a).[8]

To assign these peaks and identify all the species in this solution, systematic experiments were carried out to establish the range of ^{11}B chemical shifts to be expected for the species with the $[Zr_6BCl_{12}]^+$ core. Early ^{11}B NMR measurements upon this boron-centered cluster in basic $ImCl/AlCl_3$ ionic liquids in our laboratories showed that the cluster $[(Zr_6BCl_{12})Cl_6]^{5-}$ gave a sharp singlet at 184.0 ppm.[6] After the mixture of $Rb_5Zr_6Cl_{18}B$ and 6 equiv of $TlPF_6$ was stirred in acetonitrile for 1 day, a white solid (TlCl) was formed, and the ^{11}B NMR spectrum of the resulting orange red solution showed only one sharp singlet at 196.3 ppm (Figure 1b). Provided that six terminal chlorides were abstracted by the thallium ion and the $[Zr_6BCl_{12}]^+$ cluster core remains intact, this singlet can be attributed to $[(Zr_6BCl_{12})(NCCH_3)_6]^+$.

After establishing the chemical shifts for the two extreme species, $[(Zr_6BCl_{12})Cl_6]^{5-}$ and $[(Zr_6BCl_{12})(NCCH_3)_6]^+$, experiments were conducted to establish spectral characteristics of all other species with terminal CH_3CN and Cl^- ligands. Assuming the charge to chemical shift correlation holds no surprise and the less negatively charged cluster species are more deshielded, the weak peak far downfield (194 ppm) in Figure 1a can be reasonably assigned as $[(Zr_6BCl_{12})Cl(NCCH_3)_5]$. The next two peaks (at 192 and 191 ppm) should arise from *cis*- and *trans*-$[(Zr_6BCl_{12})Cl_2(NCCH_3)_4]^-$, and the last two weak peaks (189.7 and 189 ppm) can be attributed to the species of *fac*- and *mer*-$[(Zr_6BCl_{12})Cl_3(NCCH_3)_3]^{2-}$. When $Rb_5Zr_6Cl_{18}B$ was dissolved in acetonitrile with the addition of about 10 equiv of PPNCl, a series of four singlets was observed in the ^{11}B NMR spectrum (Figure 1c) with the chemical shifts of 188.0, 187.3, 186.1, and 185.0 ppm. The two singlets at 188.0 and 187.3 ppm correspond to *cis*- and *trans*-$[(Zr_6BCl_{12})Cl_4(NCCH_3)_2]^{3-}$, respectively. And the last two singlets (186.2 and 185.1 ppm) are due to $[(Zr_6BCl_{12})Cl_5(NCCH_3)]^{4-}$ and $[(Zr_6BCl_{12})Cl_6]^{5-}$, respectively. Thus, we can identify all 10 possible cluster species, $[(Zr_6BCl_{12})Cl_{6-x}(NCCH_3)_x]^{x-5}$ ($x = 0-6$), based on their chemical shifts in acetonitrile. Further experimentation in which chloride concentration was varied systematically revealed that peaks grew in and disappeared in a manner consistent with these assignments. We are not able to definitively differentiate *cis* vs *trans* and *fac* vs *mer* isomers, but it is likely that intensity differences reflect differences in concentrations, and that relative concentrations of isomeric species are determined by statistical factors (i.e., [*cis*] > [*trans*] and [*mer*] > [*fac*]).

Since RbCl is virtually insoluble in acetonitrile (0.0034 wt %),[24] the available chloride in a solution of $Rb_5Zr_6Cl_{18}B$ is low. It is therefore not surprising to see that cluster complexes actually observed in acetonitrile solutions of this compound show extensive solvolysis. Thus, the discrete $[(Zr_6BCl_{12})Cl_6]^{5-}$ ion is not directly extracted from the precursor solid as one might suppose, but displacement of chloride by the solvent, CH_3CN, occurs. Our study of carbon-centered clusters showed similar results.[8] It is actually difficult to prepare the cluster complexes with six terminal chlorides in acetonitrile; presumably, the high negative charge of the complex inhibits complete chloride binding. A large excess of free chloride (ca. 50 equiv of PPNCl) must be supplied to obtain an acetonitrile solution in which $[(Zr_6BCl_{12})Cl_5(NCCH_3)]^{4-}$ and $[(Zr_6BCl_{12})Cl_6]^{5-}$ are the predominant species. It is also interesting to note that the addition of either $TlPF_6$ or PPNCl promotes the dissolution of the starting material, $Rb_5Zr_6Cl_{18}B$.

(ii) Cluster in Methanol. $Rb_5Zr_6Cl_{18}B$ can be readily dissolved into anhydrous methanol to form an orange red solution while about 5−10% of the solid (presumably ZrO_xCl) remains insoluble. The ^{11}B NMR spectrum of this solution shows two singlets: one intense, sharp peak at 191.2 ppm and one weak peak at 190.3 ppm, which are assigned as $[(Zr_6BCl_{12})(CH_3OH)_6]^+$ and $[(Zr_6BCl_{12})Cl(CH_3OH)_5]$, respectively. With the addition of more chloride, these peaks were gradually attenuated and new peaks corresponding to $[(Zr_6BCl_{12})Cl_x(CH_3OH)_{6-x}]^{1-x}$ species grew in. After this

(24) Stephen, H.; Stephen, T. *Solubilities of Inorganic and Organic Compounds*; Stephen, H., Stephen, T., Ed.; Pergamon Press Limited: Oxford, 1963.

solution was left undisturbed at −20 °C for several days, orange red crystals were formed on the wall of the ampule. One of the crystals was subjected to an X-ray crystallographic study that confirmed the presence of the $[Zr_6BCl_{12}]^+$ cluster core and six methanol molecules occupying the terminal positions.[25] These crystals liquefied when the ampule was warmed to room temperature.

The addition of 6 equiv of $TlPF_6$ to the above solution leads to the disappearance of the weak singlet due to $[(Zr_6BCl_{12})Cl(CH_3OH)_5]$, and only the peak due to $[(Zr_6BCl_{12})(CH_3OH)_6]^+$ remains. Since methanol should be a more effective donor to zirconium than acetonitrile, more solvolysis occurs and $[(Zr_6BCl_{12})(CH_3OH)_6]^+$ is the major species in methanol. However, it is not clear why $[(Zr_6BCl_{12})(CH_3OH)_6]^+$ shifts 5 ppm upfield with respect to its acetonitrile analogue, $[(Zr_6BCl_{12})(NCCH_3)_6]^+$.

We were initially surprised that $[Zr_6BCl_{12}]^+$ solutions are stable in a protic solvent like methanol; we had expected cluster decomposition to occur. ($Rb_5Zr_6Cl_{18}B$ can also be readily dissolved in deoxygenated water, though decolorization of the solution that occurs within several hours at room temperature signals cluster decomposition.) We note that methanol solutions of $[(Zr_6BCl_{12})(CH_3OH)_6]^+$ (after the treatment of $TlPF_6$) slowly decompose at room temperature. White solid slowly precipitates from the clear red solution, which is the indicative of cluster decomposition and, ultimately, formation of oxidation products (perhaps via disproportionation or gradual formation of H_2). Qualitative observations suggest that the presence of free chloride in solution helps stabilize the cluster. We speculate that the terminal methanol ligands in some way move into bridging positions in a process that precedes cluster decomposition. The reactivity of bridging halides has been demonstrated for Fe-centered clusters with the observation of inner bromide−chloride exchange when $KZr_6Br_{15}Fe$ was dissolved into basic $ImCl/AlCl_3$.[4,5] Since the displacement of inner chlorides by methanol will release chloride ions to the solution, perhaps the presence of free chloride in solution helps to suppress this displacement reaction by accelerating the back reaction wherein chloride moves back into the bridging position.

We have seen that methanolic solutions of boron- or carbon-centered clusters are reasonably stable. In contrast, Be-centered clusters show significant decomposition in methanol within a few hours, as evidenced by gradual bleaching of the solutions and disappearance of resonances characteristic of such clusters in the ^9Be NMR spectrum. Clusters centered by manganese or iron decompose rapidly in methanol. The reactivities of these clusters does not correlate the measured oxidation potentials[26] or overall charge on the cluster cores, but seems to be associated with the size of the interstitial atom and, correspondingly, the size of the surrounding Zr_6 cage. Larger Zr_6 cages are more sterically accessible and are perhaps more reactive toward nucleophiles which bind (initially) at their terminal positions.

(iii) Cluster in Pyridine. At room temperature, only ∼2−3 mg of $Rb_5Zr_6Cl_{18}B$ can be dissolved in 4.0 mL of neat pyridine to yield a red solution, and most of the starting material remains undissolved. The ^{11}B NMR spectrum shows this red solution contains only the neutral cluster, $[(Zr_6BCl_{12})Cl(py)_5]$. When $TlPF_6$ was dissolved along with $Rb_5Zr_6Cl_{18}B$ into pyridine, more of the latter compound dissolves and the corresponding ^{11}B NMR spectrum shows $[(Zr_6BCl_{12})(py)_6]^+$ is the only component. More $Rb_5Zr_6Cl_{18}B$ (about 64% of the total added) can be dissolved in 4.0 mL of pyridine at 120 °C to form a more intensely colored red solution. However, two strong singlets in the ^{11}B NMR spectrum indicated that it contained not only $[(Zr_6BCl_{12})Cl(py)_5]$ but also *cis*-/*trans*-$[(Zr_6BCl_{12})Cl_2(py)_4]^-$. Only the *cis*-$[(Zr_6BCl_{12})Cl_2(py)_4]^-$ complex was isolated from this solution in single crystals. Partial cluster decomposition probably occurs with prolonged heating at higher temperature; this liberates more chloride ions into the solution to enable formation of $[(Zr_6BCl_{12})Cl_2(py)_4]^-$.

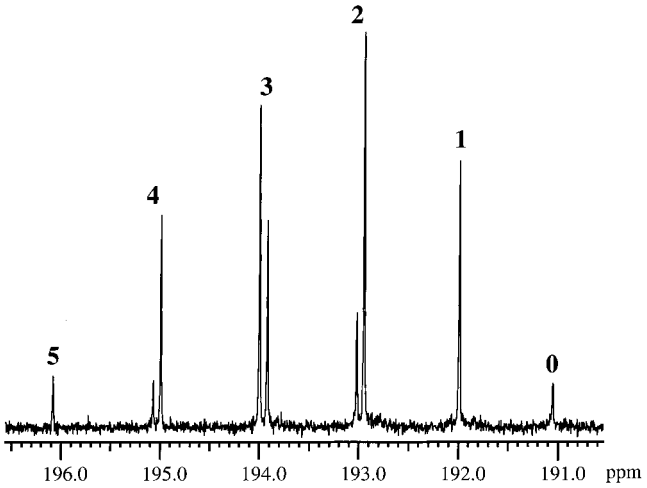

Figure 2. ^{11}B NMR spectrum of a methanol solution of $[Zr_6BCl_{12}]^+$ with the addition of pyridine, showing 9 of the 10 possible species, $[(Zr_6BCl_{12})(CH_3OH)_{6-x}(NCCH_3)_x]^+$ ($x = 0-6$). Labels are assigned values of x.

(iv) Cluster in a Mixture of Acetonitrile and Pyridine. When a small amount of pyridine was added to the acetonitrile solution of $[(Zr_6BCl_{12})(NCCH_3)_6]^+$, the ^{11}B NMR spectrum indicated that the solution was the mixture of $[(Zr_6BCl_{12})(py)_x(NCCH_3)_{6-x}]^+$ ($x = 6, 5, 4$) with no terminal chloride bound to the cluster core. However, when this solution was left in a glovebox for several days, red crystals of $[(Zr_6BCl_{12})Cl(py)_5]\cdot 3CH_3CN$ were obtained along with a gray precipitate. It is likely that the terminal chloride in the crystallized complex derives from chloride ion released by slow decomposition of the cluster.

(v) Cluster in a Mixture of Methanol and Pyridine. When pyridine (py) was added to a methanol solution of $[(Zr_6BCl_{12})(CD_3OD)_6]^+$ until the pyridine mole fraction of the solvent was 5%, the corresponding ^{11}B NMR spectrum showed the original intense singlet attributable to ($[(Zr_6BCl_{12})(CD_3OD)_6]^+$) becomes weak, and five new resonances corresponding to $[(Zr_6BCl_{12})(CD_3OD)_{6-x}(py)_x]^+$ ($x = 1-5$), respectively, appear in the ^{11}B NMR as illustrated in Figure 2. For both complexes $[(Zr_6BCl_{12})(CD_3OD)_4(py)_2]^+$ (**2**) and $[(Zr_6BCl_{12})(CD_3OD)_2(py)_4]^+$ (**4**), the statistical molar ratio of *cis* and *trans* geometric isomers is expected to be 4:1 and $[(Zr_6BCl_{12})(CD_3OD)_3(py)_3]^+$ (**3**), the mole ratio of *fac* and *mer* isomers, is statistically expected to be 2:3. The observed ratios of the integrated intensities within each pair of singlets are remarkably close to these statistical "predictions", clearly indicating that there is no significant difference in the enthalpies of the geometric isomers.

(b) Methanol−Pyridine Exchange. As the spectrum in Figure 2 clearly suggests, pyridine and methanol (CD_3OD) are a pair of neutral ligands whose cluster binding energies are similar enough that we can extract precise thermodynamic parameters describing their competitive binding. The statistical intensity ratios observed for the pairs of geometric isomers, **2**−**4**,

(25) The data set obtained for this crystal was inadequate to enable a full structure solution. Although the $[(Zr_6BCl_{12})(CH_3OH)_6]^+$ cluster was unambiguously identified and could be refined anisotropically, approximately 40% of the cell volume was occupied by solvent and/or an unidentified counteranion(s). Problems with extreme disorder prevented us from making much further progress with this data set.

(26) Sun, D.; Hughbanks, T. Unpublished results.

Table 3. Thermodynamic Data at 253 K for the Exchange Reactions ($x = 0-4$): $[(Zr_6BCl_{12})(CD_3OD)_{6-x}(py)_x]^+ + py \rightleftharpoons [(Zr_6BCl_{12})(CD_3OD)_{5-x}(py)_{x+1}]^+ + CD_3OD$

x	K_x	ΔG_x (kJ/mol)	$T\Delta S_{config,x}$ (kJ/mol)	$\Delta G_x + T\Delta S_{config,x}$ (kJ/mol)
0	79(6)	−9.2(2)	3.8	−5.4 (2)
1	36(1)	−7.53(8)	1.93	−5.60(8)
2	18.7(7)	−6.16(8)	0.61	−5.55(8)
3	10.3(5)	−4.91(9)	−0.61	−5.52(9)
4	4.9(5)	−3.3(2)	−1.93	−5.3(2)

led us to assume that the relative intensities of these peaks were proportional to the concentration of the species to which they corresponded. (This assumption is considered further below, and corrections are added as necessary.) The equilibrium constants, K_x, and corresponding free energy differences, ΔG_x , were then obtained according to eq 1 for the stepwise reactions in which methanol ligands are replaced by pyridine ($x = 0-5$): $[(Zr_6BCl_{12})(CD_3OD)_{6-x}(py)_x]^+ + py \rightleftharpoons [(Zr_6BCl_{12})(CD_3OD)_{5-x}(py)_{x+1}]^+ + CD_3OD$

$$K_x = \frac{[(Zr_6BCl_{12})(CD_3OD)_{5-x}(py)_{x+1}]^+}{[(Zr_6BCl_{12})(CD_3OD)_{6-x}(py)_x]^+} \times \frac{[CD_3OD]}{[py]} \quad (1)$$

These free energy differences are most usefully compared by canceling a configurational entropy term, $\Delta S_{config,x}$, that accounts for the combinatorial weights, W_x, which are simply the number of ways that x pyridine ligands can be placed on a cluster:

$$\Delta S_{config,x} = R \ln\left[\frac{W_{x+1}}{W_x}\right] = R \ln\left[\frac{x+1}{6-x}\right] \quad (2)$$

where the last equality follows because the weights are binomial coefficients, $W_x = 6!/x!(6\text{-}x)!$. As can be seen in the last column of Table 3, $\Delta G_x + T\Delta S_{config,x}$ is remarkably constant for all values of x. For each zirconium center of the cluster, the displacement of a methanol ligand by pyridine is independent of whether such a displacement has already occurred at another zirconium atom on the cluster.

Variable-temperature NMR experiments were performed at 20, 0, −10, −20, −30, and −40 °C to determine ΔH_x values. However, for this mixed pyridine−methanol system, van't Hoff plots ($\ln(K_x)$ vs $1/T$) yielded reasonably straight lines for only the two equilibria (K_1, K_2) involving the three most intense NMR resonances (**1**, **2**, and **3**). The values of $\Delta H_1 = -3.3 \pm 0.8$ kJ/mol and $\Delta S_1 = 16 \pm 3$ J/mol were obtained for the process involving K_1, and those of $\Delta H_2 = -2.3 \pm 0.9$ kJ/mol and $\Delta S_2 = 14 \pm 3$ J/mol were obtained for the process involving K_2. These measurements are much more sensitive to integration errors (and, perhaps, relaxation time effects—see below) than the data given in Table 3, but also indicate that the $[Zr_6BCl_{12}]^+$ core binds pyridine more strongly than methanol only by a few kJ/mol. Equilibria involving integration of weaker resonances did not yield useful data.

(c) Relaxation Times. Although thousands of boron compounds have been examined by use of ^{11}B NMR spectroscopy,[27] solution-state relaxation behavior has not been so extensively studied.[28] Even line widths, which are related to spin−spin relaxation times (T_2's) and can be readily obtained by straightforward spectroscopic measurements,[29] have only been reported for a handful of species (and T_2's are at least lower bounds for corresponding T_1's). Except under very rare circumstances, relaxation times (T_1's) observed for compounds containing the quadrupolar ^{11}B nucleus are quite short; most of the T_1 data reported in the literature were measured on polyhedral boranes, and these times range from 1 to 200 ms.[27,30] Fehlner et al. observed narrow lines (~11 Hz) and long relaxation times ($T_1 \sim 0.4$ s) for *cis*- and *trans*-$[Fe_4Rh_2B(CO)_{16}]^-$, in which the boron atom is located in an interstitial cavity of a nearly octahedral hexanuclear transition-metal cluster.[31,32] Indeed, it is in cases where high symmetry holds (e.g., T_d or O_h) or the electric field gradient at the nucleus is fortuitously small that long relaxation times (T_1's) are observed. For example, a solution of $NaBH_4$ in D_2O exhibits an exceptionally long ^{11}B relaxation time ($T_1 = 10$ s).[28]

Table 4. Spin−Lattice Relaxation Times for $[(Zr_6BCl_{12})(py)_x(CD_3OD)_{6-x}]^+$ ($x = 0-4$)

cluster ion	(T_1, seconds) 20 °C	−20 °C
cis-$[(Zr_6BCl_{12})(py)_4(CD_3OD)_2]^+$	11.8 ± 2.0	6.8 ± 0.4
mer-$[(Zr_6BCl_{12})(py)_3(CD_3OD)_3]^+$	11.6 ± 0.7	5.6 ± 0.1
fac-$[(Zr_6BCl_{12})(py)_3(CD_3OD)_3]^+$	13.5 ± 1.0	5.8 ± 0.2
trans-$[(Zr_6BCl_{12})(py)_2(CD_3OD)_4]^+$	10.4 ± 0.8	5.2 ± 0.2
cis-$[(Zr_6BCl_{12})(py)_2(CD_3OD)_4]^+$	9.2 ± 0.4	5.0 ± 0.05
$[(Zr_6BCl_{12})(py)(CD_3OD)_5]^+$	10.9 ± 0.5	4.9 ± 0.1
$[(Zr_6BCl_{12})(CD_3OD)_6]^+$	8 ± 1	4.8 ± 0.8

In our studies of $[(Zr_6BCl_{12})(CD_3OD)_{6-x}(py)_x]^+$ ($x = 1-5$) species, we noticed the very close correspondence between peak ratios in the pairs **2**, **3**, and **4** and the statistically expected isomer ratios. This fact and literature precedent initially led us to an overly naive interpretation of NMR data collected while using acquisition times of 2.5 s. We initially assumed that our peak integrations were reliable indicators of relative concentrations of cluster species because we had assumed that our acquisition times were sufficiently long to enable essentially complete relaxation of the ^{11}B spin system. As it turns out, T_1's for many ^{11}B-centered clusters are longer than 2.5 s, including T_1's measured for $[(Zr_6BCl_{12})(CD_3OD)_{6-x}(py)_x]^+$ ($x = 0-5$) species (Table 4). At ambient temperature, these relaxation times range from 8 to 13 s, with relatively large errors (±1−2 s). There seems to be a general, albeit slight, increase in the measured T_1's as the number of pyridine ligands increases. Unfortunately, these long relaxation times place a practical limit on the precision of the T_1 measurement themselves and a more detailed analysis is problematic. However, it is clear that an acquisition time of 2.5 s is not long enough to assume complete relaxation. It is, nevertheless, impractical to use ~40 s of acquisition time to collect the number of transients necessary to obtain an adequate spectrum.

Additional relaxation time measurements were performed at −20 °C. The measured T_1 values range from 4.8 to 6.8 s, and these are determined with sufficiently high precision that we can be confident that the general trend seen in the data at room temperature persists. Interestingly, there is no significant difference in measured T_1 values for the isomeric species whose resonances fall in groups of peaks in **2**, **3**, and **4**. It is therefore reasonable that when comparing integrated intensities of isomeric species, a negligible error is made by assuming the

(27) Mason, J. *Multinuclear NMR*; Plenum: New York, 1987.
(28) Pochapsky, T. C.; Wang, A.; Stone, P. M. *J. Am. Chem. Soc.* **1993**, *115*, 11084−11091.
(29) Brevard, C.; Granger, P. *Handbook of High-Resolution Multinuclear NMR*; John Wiley & Sons: New York, 1981.
(30) Kidd, R. G. *NMR of Newly Accessible Nuclei*; Academic: New York, 1983; Vol. 2.
(31) Khattar, R.; Fehlner, T. P.; Czech, P. T. *New J. Chem.* **1991**, *15*, 705−711.
(32) Rath, N. P.; Fehlner, T. P. *J. Am. Chem. Soc.* **1988**, *110*, 5345−5349.

Table 5. Spin−Lattice Relaxation Times (T_1's) for Several Cluster Species at 20 °C

species	T_1 (s)	species	T_1 (s)
$[(Zr_6BCl_{12})(NCCH_3)_6]^+$	108 ± 5	$[(Zr_6BCl_{12})Cl(NCCH_3)_5]$	0.452 ± 0.008
$[(Zr_6BCl_{12})(py)_6]^+$	32.9 ± 1.7	$[(Zr_6BCl_{12})Cl_2(NCCH_3)_4]^-$	0.432 ± 0.006
$[(Zr_6BCl_{12})(CD_3OD)_6]^+$	15.4 ± 0.3	$[(Zr_6BCl_{12})Cl(py)_5]$	0.200 ± 0.001
$[(Zr_6BCl_{12})Cl(CH_3OH)_5]$	0.88 ± 0.03	$[(Zr_6BCl_{12})Cl_2(py)_4]^-$	0.239 ± 0.006

intensities are proportional to concentrations. Making the assumption that the nuclear magnetization conforms to the Bloch equations, the intensity observed for a given resonance (I_A) should be proportional to the extent to which the pulse induced magnetization decays to its equilibrium value:[33]

$$I_A \propto (M_0 - M_z(0))(1 - e^{-\tau/T_{1A}}) \quad (3)$$

where M_0 is the equilibrium longitudinal magnetization, $M_z(0)$ is the longitudinal magnetization after the perturbing pulse, t is the acquisition time, and T_{1A} is the spin−lattice relaxation time for nucleus A. Knowing the relaxation times, we can make corrections to our naive interpretation of the spectrum in Figure 2 by calculating the concentration ratios of any two species, A and B, after accounting for the influence of differences in these species' relaxation times:

$$\frac{[A]}{[B]} = \frac{I_A}{I_B}\frac{1 - e^{-\tau/T_{1B}}}{1 - e^{-\tau/T_{1A}}} \quad (4)$$

The corrections implied by the second factor in this expression were applied to all the entries but the last in Table 3 (we do not have an accurate relaxation time for $[(Zr_6BCl_{12})(py)_5(CD_3OD)]^+$). Because the range of relaxation times is small, none of these corrections changes ΔG_x values computed solely from intensity ratios by more than 0.3 kJ/mol.

For other boron-centered zirconium halide clusters, we observe similarly remarkable T_1's. The results of several such measurements are shown in Table 5. This table clearly shows that the T_1's are particularly long for the "homoleptic" species, $[(Zr_6BCl_{12})L_6]^+$ (L = py, CH_3OH, CH_3CN). The value of 108 s for $[(Zr_6BCl_{12})(NCCH_3)_6]^+$ is the longest relaxation time (T_1) ever reported for ^{11}B. In these symmetrical molecules, the boron atom sits in a perfect octahedral environment and the electric field gradient (*eq*) at the nucleus is virtually zero. The relaxation times decrease markedly for the lower-symmetry, mixed-ligand complexes, $[(Zr_6BCl_{12})Cl_xL_{6-x}]^{1-x}$ (L = py, CH_3CN, and CH_3OH; $x = 1, 2$), in which the boron atom feels nonzero electric field gradients. Of course, even for these species, the measured T_1's are considerably longer than are found for almost all conventional boron compounds. One anomaly should be noted: T_1 measured for $[(Zr_6BCl_{12})(CD_3OD)_6]^+$ in mixed py-CD_3OD is 8 ± 1 s at 20 °C—significantly shorter than the value of 15.4 ± 0.3 s measured for the same species when $Rb_5Zr_6Cl_{18}B$ was dissolved in pure methanol (Table 5). We do not understand this apparent discrepancy since the pyridine mole fraction in the mixed solvent system is only 5%.

We have often observed poor signal-to-noise ratios for ^{13}C resonances when studying carbon-centered clusters, $[(Zr_6{}^{13}CCl_{12})^{2+}L_6]$, despite full ^{13}C enrichment in cluster synthesis.[8] The long relaxation times we have observed for $[(Zr_6{}^{11}BCl_{12})]^+$ species, especially when they are symmetrically ligated, suggests that the spin−lattice relaxation times (T_1) for ^{13}C-centered clusters may be extremely long indeed. The species $[(Zr_6{}^{13}CCl_{12})(NCCH_3)_6]^{2+}$ is somewhat difficult to detect and the "$(Zr_6{}^{13}CCl_{12})^{2+}$" ion gives an exceedingly weak signal when observed in an acidic $ImCl/AlCl_3$ ionic liquid.[8] Although we have not yet measured relaxation times for ^{13}C-centered clusters, it seems likely that with quadrupolar relaxation entirely absent as a mechanism, T_1's are likely to be quite long, and this will continue to present some practical difficulties in the use of NMR in studying C-centered clusters.

(d) $^{11}B-^{31}P$ Coupling. Assuming certain line broadening mechanisms (e.g., exchange, coupling, field inhomogeneity) can be neglected, the spin−spin relaxation time (T_2) is associated with the full width of the NMR line at half-height ($\Delta\nu_{1/2}$): $\Delta\nu_{1/2} = 1/(\pi T_2)$, and T_1 is an upper limit on the value of T_2 ($T_2 \leq T_1$).[29] The efficient relaxation and shortened T_1's characteristic of the ^{11}B nucleus by virtue of its quadrupole moment result in broadened ^{11}B NMR signals ($\Delta\nu_{1/2} > 10$ Hz). This prevents the observation of coupling constants much less than 10 Hz for ^{11}B spectra. In an exceptional example, $C_5H_5BeBH_4$, a half-height width ($\Delta\nu_{1/2} = 1.5$ Hz) comparable to B-centered hexazirconium clusters, was observed.[34] In that example, a $^9Be-^{11}B$ coupling constant of 3.7 Hz was observed in the ^{11}B NMR spectrum.

Most data available for ^{11}B spectra involve adjacent nuclei; two-bond coupling constants tend to be smaller and are less commonly observed. One-bond $^{11}B-^{31}P$ coupling constants exhibit a rather wide range of variation (13 to 217 Hz).[35] Two-bond $^{31}P-^{11}B$ coupling constants are only rarely observed. The first two-bond coupling constant, $^2J(^{11}B-^{31}P) = 13.75$ Hz, was directly observed in the ^{11}B NMR spectrum of $N(PCl_2NMe)_2BCl_2$.[36] Spencer et al. reported $^2J_{PBB}$ coupling constants of 18 and 19 Hz, measured in 2D COSY NMR cross-peaks, which were unresolved in the corresponding 1D ^{11}B NMR spectrum.[37] We observe remarkably narrow lines ($\Delta\nu_{1/2}$: 0.3−3.0 Hz) for boron-centered zirconium halide cluster complexes. (In fact, the observed half-height line width of 0.3 Hz for $[(Zr_6BCl_{12})(NCCH_3)_6]^+$ is only an upper bound on the real line width because the digital resolution of the instrument proved to be limiting.) We shall see that coupling constants as small as 1.9 Hz are clearly resolved in the 1D ^{11}B NMR spectra of some cluster complexes.

When excess triethylphosphine (PEt_3) was added into an acetonitrile solution of $[(Zr_6BCl_{12})(NCCH_3)_6]^+$, several multiplets attributable to a $[(Zr_6BCl_{12})(NCCH_3)_{6-x}(PEt_3)_x]^+$ (x = 2−6) mixture were observed in the ^{11}B NMR spectrum. However, the spectrum was quite complex and definitive assignments of those resonances could not be simply made. When the acetonitrile solvent was removed by evacuation, the resulting red solid could be dissolved in dichloromethane to form a red solution. This solution yields a pleasing septet at 199 ppm ($^2J(^{11}B-^{31}P) = 8.8$ Hz) in the ^{11}B spectrum that is clearly attributable to $[(Zr_6BCl_{12})(PEt_3)_6]^+$ (Figure 3a). The same coupling constant is also observed in the corresponding

(33) Canet, D. *Nuclear Magnetic Resonance: Concepts and Methods*; John Wiley & Sons: Chichester, 1996.

(34) Gaines, D. F.; Walsh, J. L.; Morris, J. H.; Hillenbrand, D. F. *Inorg. Chem.* **1978**, *17*, 1516−1522.

(35) Noth, H.; Wrackmeyer, B. *Nuclear Magnetic Resonance Spectroscopy of Boron Compounds*; Springer: Berlin, 1978; Vol. 14.

(36) Binder, H.; Palmtag, J. *Z. Naturforsch., Teil B* **1979**, *34*, 179−187.

(37) Spencer, J. T.; Goodreau, B. H. *Inorg. Chem.* **1992**, *31*, 2612−2621.

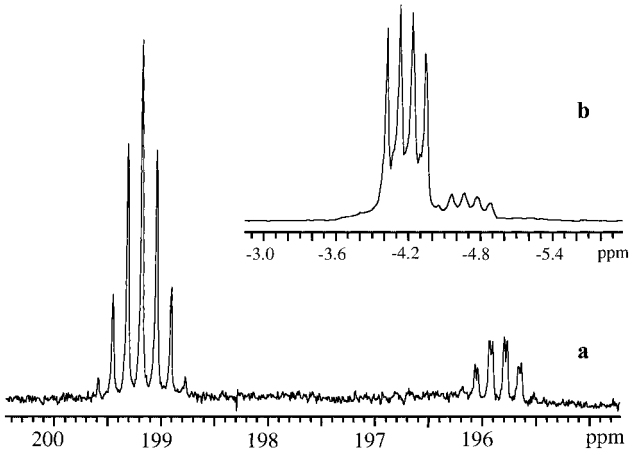

Figure 3. (a) ^{11}B NMR spectrum of PEt_3 complexes of the $[Zr_6BCl_{12}]^+$ cluster in CH_2Cl_2. (b) ^{31}P NMR spectrum for the same sample in (a).

^{31}P NMR spectrum (Figure 3b) where a quartet with equal line intensities is expected for coupling to ^{11}B ($I = 3/2$, 81%). Underlying this quartet is a septet due to splitting by the ^{10}B isotope ($I = 3$, 19% abundance).

Besides the intense septet in the ^{11}B spectrum, a weaker sextet is observed near 195 ppm with an 8.8 Hz coupling constant. Each peak of this sextet is further split into a doublet with a 1.9 Hz coupling constant. In the corresponding ^{31}P NMR spectrum, a weak multiplet resonance is visible near the intense quartet. Since phosphine oxides are common impurities in organic phosphines, we assign this species as $[(Zr_6BCl_{12})(OPEt_3)(PEt_3)_5]^+$, assuming that the boron atom couples with the phosphorus atom of the terminal $OPEt_3$ through three bonds (P−O−Zr−B). The ^{31}P NMR spectrum of the PEt_3 used in this reaction confirms that it contains approximately 0.6 mol % $OPEt_3$—a surprisingly small fraction in view of the ^{11}B NMR spectrum in Figure 3 where it appears that the multiplet associated with $[(Zr_6BCl_{12})(OPEt_3)(PEt_3)_5]^+$ has an intensity that is roughly 25% as large as that for $[(Zr_6BCl_{12})(PEt_3)_6]^+$. This disproportionate intensity may mean that the oxo-donor, $OPEt_3$, binds more effectively to $[Zr_6BCl_{12}]^+$ than PEt_3. Such a preference would be reasonable given the oxophilicity of zirconium and the smaller steric requirements of the $OPEt_3$ ligand. However, we have not ruled out the possibility that the relative intensity of the septet due to $[(Zr_6BCl_{12})(PEt_3)_6]^+$ is reduced because this more symmetrical species has a longer relaxation time.

This three-bond coupling ($^3J_{P-O-Zr-B}$) between boron and phosphorus can also be observed in an experiment conducted with triphenylphosphine oxide ($OPPh_3$). When approximately 6 equiv of triphenylphosphine oxide ($OPPh_3$) were added into the pyridine solution of $[(Zr_6BCl_{12})(py)_6]^+$, an intense doublet due to $[(Zr_6BCl_{12})(OPPh_3)(py)_5]^+$ and an intense triplet due to *cis*- or *trans*-$[(Zr_6BCl_{12})(OPPh_3)_2(py)_4]^+$ both exhibit 1.9 Hz splittings in the ^{11}B spectrum (Figure 4). A weaker, poorly resolved triplet at 193.2 ppm is probably due to the second isomer of *cis*-, *trans*-$[(Zr_6BCl_{12})(OPPh_3)_2(py)_4]^+$. Two weak quartet-like resonances around 191 ppm can be attributed to *fac*-, *mer*-$[(Zr_6BCl_{12})(OPPh_3)_3(py)_3]^+$. The weak, sharp singlet at 196.6 ppm arises from the starting material, $[(Zr_6BCl_{12})(py)_6]^+$. The chemical shift trend for phosphine oxides seems to be quite similar to those we have seen for chloride; the boron atom becomes less deshielded as more OPR_3 ligands are bound to the cluster.

When excess triphenylphosphine (PPh_3) was added into an acetonitrile solution of $[(Zr_6BCl_{12})(NCCH_3)_6]^+$, the ^{11}B NMR

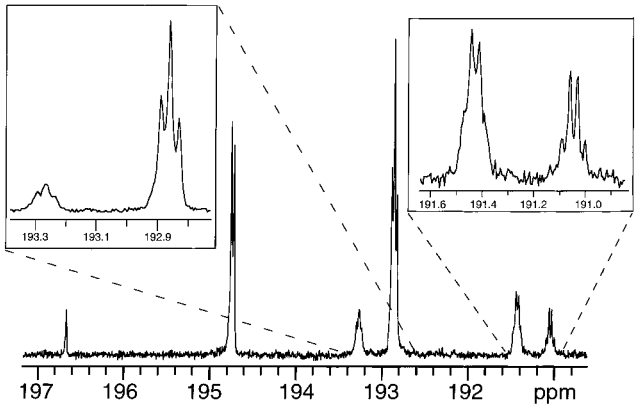

Figure 4. ^{11}B NMR spectrum of a pyridine solution of $[Zr_6BCl_{12}]^+$ with the addition of $OPPh_3$. The doublet, triplet, and quartet are attributed to $[(Zr_6BCl_{12})(py)_5(OPPh_3)]^+$, $[(Zr_6BCl_{12})(py)_4(OPPh_3)_2]^+$, and $[(Zr_6BCl_{12})(py)_3(OPPh_3)_3]^+$, respectively. Insets show the triplets and the quartets more clearly.

spectrum does not change, indicating that triphenylphosphine does not bind to the cluster core. Each zirconium atom resides well inside the basal plane formed by the four chloride ligands to which it is bound, and the steric exclusivity this confers on the cluster apparently prohibits this bulkier phosphine (145° cone angle)[38,39] from binding to the cluster.

Phosphines (PR_3) do not coordinate particularly well to the $[Zr_6BCl_{12}]^+$ cluster core. Both steric and electronic factors are important. Nestling of the zirconium atoms within the cluster faces precludes binding of bulky phosphines and may contribute to weakening of Zr−P bonds even for phosphines with smaller cone angles. Phosphines may also be comparatively weak donors when in competition with "harder" N-donor or O-donor ligands. We have, for example, conducted preliminary experiments with the potentially polybasic ligand, 1,3,5-triaza-7-phosphaadamantane (PTA). PTA is a small cone angle phosphine (102°)[39] and binds solely through the phosphorus atom in complexes with palladium, for example.[40] However, preliminary NMR evidence indicates that both phosphorus and nitrogen atoms in PTA ligate the $[Zr_6BCl_{12}]^+$ cluster. This is probably best described as a manifestation of an electronic preference for nitrogen. The weakness of binding to PEt_3 is exemplified by its failure to completely displace solvent acetonitrile when an excess PEt_3 was added into an acetonitrile solution; a mixture of $[(Zr_6BCl_{12})(NCCH_3)_{6-x}(PEt_3)_x]^+$ ($x = 2-6$) was observed by ^{11}B NMR. In contrast, trialkylphosphine oxides are much stronger coordinating ligands toward the cluster core because they have minimal steric requirements and zirconium exhibits its usual oxophilicity.

(e) Crystal Structure. $[(Zr_6BCl_{12})Cl(py)_5]\cdot 3CH_3CN$ crystallizes in the orthorhombic space group *Pbcm* with 4 clusters per unit cell. The $[(Zr_6BCl_{12})Cl(py)_5]$ cluster is bisected by a mirror plane that passes through the terminal chloride (Cl3) and one pyridine ligand (N1, C11−C15). A thermal ellipsoid diagram of the cluster is shown in Figure 5. Selected bond distances and bond angles are listed in Table 6.

It has been found that the Zr−Zr and Zr−B bond distances in these boron-centered zirconium chloride clusters are strongly determined by the number of cluster bonding electrons (CBEs).[1−3,6,7] The average Zr−Zr and Zr−B bond distances in $[(Zr_6BCl_{12})(py)_5Cl]\cdot 3CH_3CN$ are 3.2609(15) Å and 2.308-

(38) Tolman, C. A. *Chem. Rev.* **1977**, *77*, 313−348.
(39) Delerno, J. R.; Trefonas, L. M.; Darensbourg, M. Y.; Majeste, R. J. *Inorg. Chem.* **1976**, *15*, 816−819.
(40) Decuir, T. J. Ph.D Thesis, Texas A&M University, 1997.

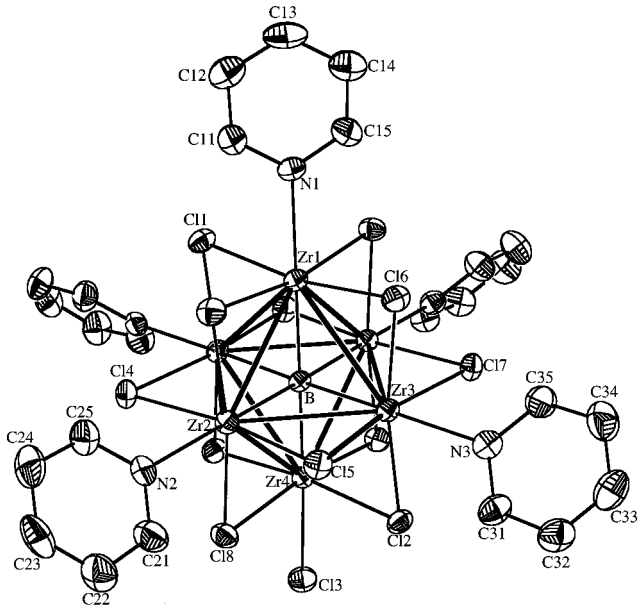

Figure 5. Molecular structure of $[(Zr_6BCl_{12})Cl(py)_5]$. Thermal ellipsoids are shown at the 50% probability level. Hydrogen atoms have been omitted for clarity.

Table 6. Selected Bond Lengths [Å] and Angles [deg] for $[(Zr_6BCl_{12})Cl(py)_5]\cdot 3CH_3CN$[a]

Zr(1)−Zr(2)	3.2380(12)	Zr(1)−B	2.319(13)
Zr(1)−Zr(3)	3.2457(12)	Zr(2)−B	2.300(9)
Zr(2)−Zr(2A)	3.262(2)	Zr(3)−B	2.301(9)
Zr(2)−Zr(3)	3.2446(10)	Zr(4)−B	2.314(13)
Zr(3)−Zr(3A)	3.261(2)		
		Zr(1)−N(1)	2.422(9)
Zr(4)−Zr(2)	3.2855(12)	Zr(2)−N(2)	2.422(7)
Zr(4)−Zr(3)	3.2895(12)	Zr(3)−N(3)	2.429(7)
av Zr−Cl[i]	2.558(2)	range: 2.546(2)−2.575(2)	
Zr(4)−Cl[a](3)	2.576(3)		

Cl(6)−Zr(1)−Cl(1)	168.77(8)	Zr(4)−B−Zr(1)	179.7(6)
Cl(1A)−Zr(2)−Cl(8)	168.58(7)	Zr(3A)−B−Zr(2)	178.3(6)
Cl(5)−Zr(2)−Cl(4)	168.85(7)	Zr(2A)−B−Zr(3)	178.3(6)
Cl(6)−Zr(3)−Cl(2)	168.97(7)	B−Zr(1)−N(1)	179.9(4)
Cl(5)−Zr(2)−Cl(7)	168.73(7)	B−Zr(2)−N(2)	178.7(3)
		B−Zr(3)−N(3)	179.0(4)
Cl(2)−Zr(4)−Cl(8A)	171.11(8)	B−Zr(4)−Cl[a](3)	178.0(3)
av Zr−B−Zr	90.0(4)	range: 89.0(4)−90.9(4)	

[a] Symmetry transformations used to generate equivalent atoms: *A*, *x*, *y*, $-z + {}^3/_2$.

(13) Å, respectively. These values are in good agreement with previously reported cluster compounds which have 14 CBEs.[6] The metal−metal bonds associated with Zr4, which is the zirconium atom bound to a terminal chloride ion, are about 0.02−0.05 Å longer than the other metal−metal bonds in the cluster. The trans $Cl^i-Zr-Cl^i$ bond angles are larger for the Zr4 atom, indicating that Zr4 is closer to the plane formed by the four bridging chloride atoms to which it is bound than are the other zirconium atoms. Similar phenomena were observed in the hydrogen-containing cluster $[(Zr_6H_4Cl_{12})Cl_2(PR_3)_4]$.[41] This small cluster distortion of the Zr_6 octahedron probably arises from the disparate electron donating ability of the terminal ligands.

The compound $[pyH]\{cis\text{-}[(Zr_6BCl_{12})(py)_4Cl_2]\}\cdot 3py$ crystallizes in the monoclinic space group *C*2/*c* with 4 cluster molecules per unit cell. The $cis\text{-}[(Zr_6BCl_{12})(py)_4Cl_2]^-$ cluster is centered on a 2-fold axis and the two terminal chlorides are

(41) Wojtczak, W. A. Ph.D. Thesis, Texas A&M University, 1993.

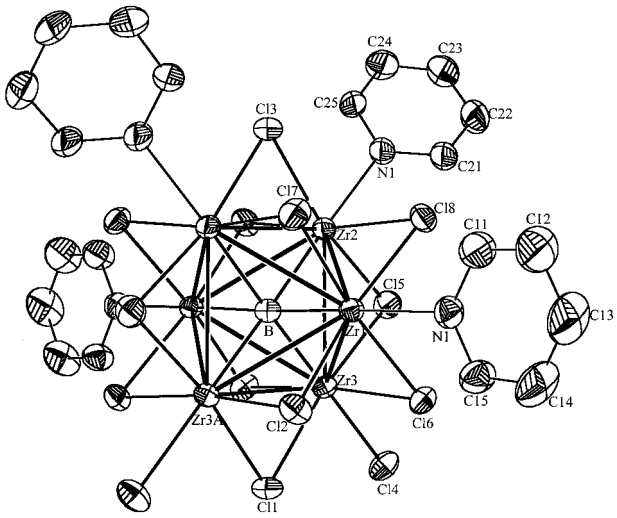

Figure 6. Structure of the $cis\text{-}[(Zr_6BCl_{12})Cl_2(py)_4]^-$ ion. Thermal ellipsoids are shown at the 50% probability level. Hydrogen atoms have been omitted for clarity.

Table 7. Selected Bond Lengths [Å] and Angles [deg] for $[pyH]\{cis\text{-}[(Zr_6BCl_{12})Cl_2(py)_4]\}\cdot 3py$[a]

Zr(1)−Zr(2)	3.2265(7)	Zr(1)−B	2.2948(5)
Zr(1)−Zr(2A)	3.2435(7)	Zr(2)−B	2.314(6)
Zr(2)−Zr(2A)	3.2181(11)	Zr(3)−B	2.305(6)
Zr(3A)−Zr(1)	3.2758(7)		
Zr(3)−Zr(1)	3.2754(7)	Zr(1)−N(1)	2.431(4)
Zr(3)−Zr(2)	3.2717(7)	Zr(2)−N(2)	2.424(5)
Zr(3)−Zr(3A)	3.3024(10)		
av Zr−Cl[i]	2.553(2)	range: 2.5391(14)−2.5647(14)	
Zr(3)−Cl[a](4)	2.594(2)		

Cl(2)−Zr(1)−Cl(8)	168.21(5)	B−Zr(1)−N(1)	178.7(3)
Cl(6)−Zr(1)−Cl(7)	168.71(5)	B−Zr(2)−N(2)	177.8(2)
Cl(5)−Zr(2)−Cl(3)	168.10(5)	B−Zr(3)−Cl[a](4)	178.61(12)
Cl(8)−Zr(1)−Cl(7A)	168.44(5)	Zr(1A)−B−Zr(1)	177.8(5)
		Zr(3A)−B−Zr(2)	178.3(3)
Cl(1)−Zr(3)−Cl(5)	171.10(5)	Zr(2A)−B−Zr(3)	178.3(3)
Cl(2A)−Zr(3)−Cl(6)	171.26(5)		
av Zr−B−Zr	90.0(2)	range: 88.2(3)−91.4(3)	

[a] Symmetry transformations used to generate equivalent atoms: *A*, $-x + 2$, *y*, $-z + {}^1/_2$.

related by this 2-fold axis. A thermal ellipsoid drawing of the cluster unit is shown in Figure 6 and selected bond distances and angles are listed in Table 7. There is one-half of a cluster $([Zr_3BCl_7(py)_2]\cdot 2py)$ per asymmetric unit, with one of the free pyridine molecules being severely disordered. The average Zr−Zr and Zr−B bond distances (3.2591(9) and 2.305(6) Å, respectively) strongly suggest that the cluster core has 14 CBEs, and therefore bears a negative charge (i.e., $[(Zr_6BCl_{12})(py)_4Cl_2]^-$). The absence of any electron density that would allow for an additional cation in the structure leads us to posit the pyridinium ion (pyH^+) as the most plausible counterion. This hypothesis also seems most consistent with the preparation of the cluster; only the Rb^+ ion might otherwise be expected to be present. It is conceivable that the presence of both pyridine molecules and pyridinium ions in the structure is associated with the severe disorder problem at one site. Even in the absence of disorder, it is unlikely that pyH^+ could be distinguished from pyridine by use of X-ray diffraction. We therefore sought to confirm that the cluster is indeed a diamagnetic (unoxidized) cluster with 14 CBEs. Eight milligrams of the crystalline product was redissolved into 3.0 mL of neat pyridine. The ^{11}B NMR spectrum of the resulting solution was identical to that of the original mother solution that contained *cis-/trans*-$[(Zr_6BCl_{12})(py)_4$-

$Cl_2]^-$ and $[(Zr_6BCl_{12})(py)_5Cl]$; none of the resonances showed significant broadening (line widths were 2.5 Hz). Other research in our laboratory has shown that the presence of oxidized (paramagnetic) clusters leads to significant ^{11}B line broadening due to outer-sphere intercluster electron-transfer reactions.[42,43] NMR evidence thus supports the formulation of this cluster as an unoxidized monoanion, but we have no *direct* evidence for the presence of pyridinium ions. The source of the protons is also not clear, but we presume that they originate from water as an impurity. From a purely technical point of view, the refinement model is reasonably good. On balance, we believe that $[pyH]\{cis\text{-}[(Zr_6BCl_{12})(py)_4Cl_2]\}\cdot 3py$ is the most plausible formula of the compound for which we have isolated crystals, even if the crystals isolated represent only a modest fraction of the solution from which they crystallized.

Just as we saw for the cluster with one terminal chloride, the two zirconium atoms bound to terminal chlorides (Zr3 and Zr3A) exhibit bonds to neighboring metal atoms that are appreciably longer (ca. 0.03−0.085 Å) than the other metal−metal bonds in the $cis\text{-}[(Zr_6BCl_{12})(py)_4Cl_2]^-$ cluster. The distance between Zr3 and Zr3A (3.3024(10) Å) is the longest in the cluster. The trans $Cl^i-Zr-Cl^i$ bond angles reveal that Zr3 is closer to the plane formed by its four bridging chloride ligands than the other zirconium atoms. The $Zr3-Cl^a$ bond distance (2.594(2) Å) is 0.04 Å longer than the average bond distance of $Zr-Cl^i$.

Conclusions

^{11}B NMR spectroscopy is a powerful analytical tool for studying boron-centered zirconium chloride clusters in solution. Remarkably long spin−lattice relaxation times (T_1's) permit the routine observation of very narrow ^{11}B resonances and rarely observed coupling constants $^2J(^{11}B-^{31}P)$ and $^3J(^{11}B-^{31}P)$ are reported. Chemical shifts or shift ranges have now been established for the boron-centered cluster species $[(Zr_6BCl_{12})X_{6-n}Y_n]$ (X, Y = MeCN, MeOH, py, PR_3, OPR_3, Cl; $n = 0-6$). ^{11}B NMR spectroscopy was also used to study the thermodynamics associated with the methanol−pyridine ligand competition for the $[(Zr_6BCl_{12})]^+$ cluster core. Furthermore, qualitative observations establish that the binding strength of neutral ligands to the $[Zr_6BCl_{12}]^+$ cluster core decreases in the following order: $OPR_3 > NC_5H_5 > CH_3OH > PR_3 > CH_3CN$. ($PR_3$ must be a phosphine with a small cone angle.) Binding of oxo-ligands, such as CH_3OH or OPR_3, seems to be favored. NMR spectroscopy provides a much needed compliment to X-ray diffraction in revealing the nature of the coordination chemistry of these clusters. The coordination chemistry and NMR spectroscopy of other centered, hexanuclear zirconium clusters, $[(Zr_6ZCl_{12})]^{n+}$ (Z = Be, C, N, Mn), are currently underway in our laboratory.

Acknowledgment. We gratefully acknowledge the Robert A. Welch Foundation for its support through Grant No. A-1132 and the National Science Foundation for its support through Grant No. CHE-9623255. We extend our thanks to Dr. Richard Staples for collecting the single crystal X-ray data set using a CCD-equipped X-ray diffractometer at Harvard University, purchased through NIH Grant No. 1S10RR11937-01.

Supporting Information Available: Figures and tables of NMR spectral data (4 pages, print/PDF). See any current masthead page for ordering information and Web access instructions. X-ray crystallographic files are available in CIF format.

JA981736N

(42) Harris, J. D. Ph.D Thesis, Texas A&M University, 1997.
(43) Harris, J. D.; Sun, D.; Hughbanks, T. Unpublished results.